References

1 LEE, K., SHUR, M., LEE, K.W., VU, T., ROBERTS, P., and HELIX, M.: 'A new interpretation of 'end' resistance measurements', *IEEE Electron. Device Lett.*, 1984, **EDL-5**, pp. 5–7

2 LEE, K.W., LEE, K., SHUR, M., VU, T., ROBERTS, P., and HELIX, M.: 'Source, drain, and gate series resistances and electron saturation velocity in ion-implanted GaAs FETs', *IEEE Trans.*, 1985, **ED-32**, pp. 987–992

3 ALAMO, J., and AZZAM, W.: 'A floating-gate transmission-line model technique for measuring source resistance in heterostructure field-effect transistors', *IEEE Trans.*, 1989, **ED-36**, pp. 2386–2393

4 FUKUI, H.: 'Determination of the basic device parameters of a GaAs MESFET', *Bell Syst. Tech.*, 1979, **58**, pp. 711–797

5 POUVIL, P., ZEMOUR, B., PASQUET, D., and GAUBERT, J.: 'Determination of source and drain parasitic resistances of HEMTs', *Electron. Lett.*, 1992, **28**, pp. 618–619

6 HOLMSTROM, R., BLOSS, W., and CHI, J.: 'A gate probe method of determining parasitic resistance in MESFETs', *IEEE Electron. Device Lett.*, 1986, **EDL-7**, pp. 410–412

7 LIU, S., FU, S., THURAIRAJ, M., and DAS, M.: 'Determination of source and drain series resistances of ultra-short gate-length MODFETs', *IEEE Electron. Device Lett.*, 1989, **EDL-10**, pp. 85–87

Direct measurement of doping density and barrier lowering effect with bias in quantum wells

Y. Xu, A. Shakouri, A. Yariv, T. Krabach and S. Dejewski

Indexing terms: Semiconductor doping, Semiconductor quantum wells, Infra-red detectors

An experimental method for determining the doping density in thin-sheet semiconductor material such as quantum wells (QWs) is demonstrated in GaAs/AlGaAs multiquantum-well infra-red photodetectors. The results agree very well with the conventional Hall measurement method. Barrier lowering effect with bias in QWs is determined experimentally.

Doping in quantum wells is a major parameter in determining their performance in various device configurations. There are several standard ways [1] of measuring doping density for bulk semiconductor material. However, direct experimental measurement of doping density in thin sheet like quantum wells has not been presented to date. In this Letter we demonstrate an experimental method for determination of doping density in quantum wells. The experimental results are compared with results from the conventional Hall measurement method.

The doping density calculation for quantum wells is straightforward. The two-dimensional (2-D) carrier density can be expressed as

$$N_{2D} = \int \rho_{2D} f(E) dE \qquad (1)$$

where ρ_{2D} is the 2-D density of states and $f(E)$ is the Fermi-Dirac distribution. If the quantum well is narrow enough such that there is only one bound state inside the well, then eqn. 1 assumes the simple form

$$N_{2D} = \frac{m^* k_B T}{\pi \hbar^2} \log(1 + e^{(E_f - E_o)/k_B T}) \qquad (2)$$

where m^* is the carrier effective mass, k_B is the Boltzmann constant, T is temperature, E_f is the Fermi energy level and E_o is the carrier ground state energy in the well.

The doping density can be determined according to eqn. 2 if the Fermi energy is determined. This can be achieved in quantum-well infra-red photodetectors (QWIP) by measuring the dark-current temperature dependence and the detector cutoff wavelength. As an example of this method, a stack of 40GaAs/AlGaAs multiquantum wells (MQWs) is grown by molecular beam epitaxy (MBE) on (100) semi-insulating GaAs substrate. The structure consists of, from the substrate to the surface, a 0.6μm n^+ GaAs bottom contact layer, 40 periods of 5.3nm GaAs well layers sandwiched by 44nm $Al_{0.24}Ga_{0.76}As$ barrier layers, and a 0.3μm n^+ GaAs top contact layer. The centre 4.7nm in each well is uniformly doped with Si. Following the MBE growth, circular mesas of 200μm diameter were defined by wet chemical etching. Au/Ni/AuGe deposited on to the top and bottom n^+ GaAs layers, liftoff and alloying techniques were used to make ohmic contact. Owing to the well known intersub-band transition selection rule, a 45° mirror was polished on the edge of the sample to couple incident infra-red radiation.

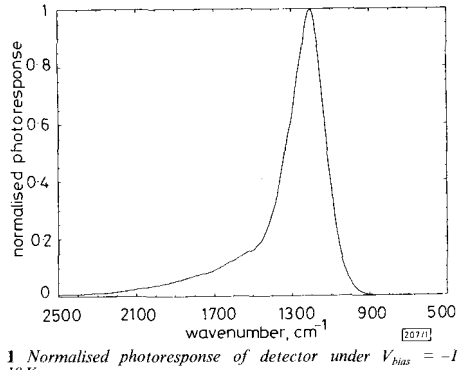

Fig. 1 *Normalised photoresponse of detector under $V_{bias} = -1V$ at $T = 10K$*

Bias polarity is defined as bottom contact is ground

These devices have a peak in the photoresponse spectrum at 1207cm^{-1}, as shown in Fig. 1. The long wavelength cutoff frequency (frequency at half-peak strength) is 1118 cm^{-1} (i.e. $E_b - E_o = 1118\,\text{cm}^{-1}$). Fig. 2 shows the dark current as a function of voltage at different temperatures.

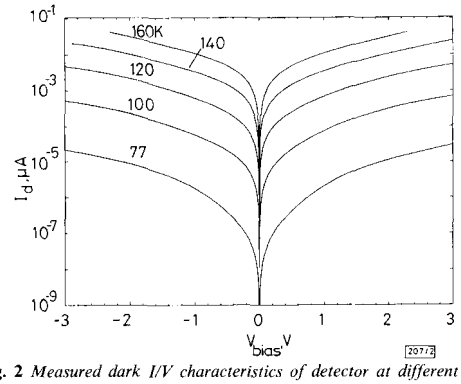

Fig. 2 *Measured dark I/V characteristics of detector at different temperatures*

The dark current for QWIP can be expressed as

$$I_d = A n_t e v_d \qquad (3)$$

where A is the device area, n_t is the carrier density contributing to the dark current, and v_d is the electron drift velocity. The thermally excited carrier density n_t is given by [2, 3]

$$n_t = \frac{1}{L_p} \int_{E_o}^{\infty} T(E,V) f(E) \rho_{2D}(E) dE \qquad (4)$$

where L_p is the MQW period, $T(E,V)$ is the transmission coefficient for an electron with energy E tunnelling through the barrier and $f(E)$ is the Fermi-Dirac distribution function. If we consider an effective barrier with potential E_b varying with bias and approximate $T(E,V)$ by $T(E,V) = 0$ for $E < E_b$ and $T(E,V) = 1$ for $E > E_b$, then eqn. 4 becomes

$$n_t = \frac{m^* k_B T}{\pi \hbar^2 L_p} \log(1 + e^{-(E_b - E_f)/k_B T}) \qquad (5)$$

When the temperature is sufficiently high (but low enough such

that $k_BT << (E_b - E_f)$), the dark current will be dominated by thermally excited carriers. Substituting eqn. 5 into eqn. 3,

$$-\log\left(\frac{I_d}{T}\right) \propto \frac{E_b - E_f}{k_BT} \qquad (6)$$

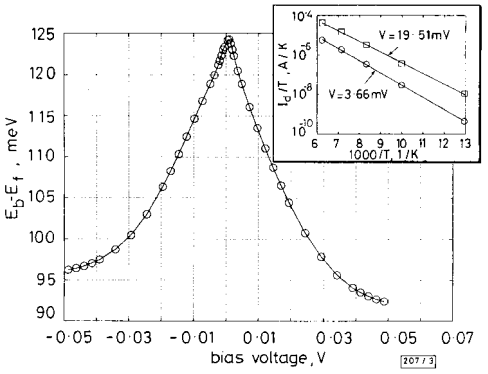

Fig. 3 *Effective barrier height seen by electrons going out of quantum wells ($E_b - E_f$) against voltage per period*

Inset: normalised dark current (I_d/T) against inverse temperature for two values of applied bias per period.
O experimental data
$E_b - E_f$ is calculated from slope of straight line for each bias

In Fig. 3, the inset plot shows the normalised dark current (I_d/T) as a function of inverse temperature for two different voltages. It can be seen that the line fitting is very good over four orders of magnitude of current change. The line slope corresponds to ($E_b - E_f$) for a given bias voltage. ($E_b - E_f$) is plotted as a function of voltage drop per period (V) in the same Figure. As expected, the effective barrier height seen by electrons going out of the quantum well is decreasing as the applied bias increases. But it does not show linear dependence [5], in contrast to the recent study by Lee *et al.* [6]. This barrier-lowering effect, which has been introduced phenomenologically by Levine *et al.* [4] to explain carrier escape probability out of the quantum wells under different biases, is thus measured directly. In addition, the peak position is not at 0V bias, which is due to the growth asymmetry [6]. From Fig. 3, the potential difference from the effective barrier to Fermi level ($E_b - E_f$) is measured to be 124meV. So, $E_f - E_0 = (E_b - E_0) - (E_b - E_f) =$ 14.6meV (using the ($E_b - E_0$) value determined by the photoresponse spectrum). From eqn. 3, $N_{2\text{-}D} = 4 \times 10^{11}\text{cm}^{-2}$. The three-dimensional density $N_{3\text{-}D}$ is then calculated to be $0.85 \times 10^{18}\text{cm}^{-3}$.

The doping density is $0.86 \times 10^{18}\text{cm}^{-3}$ from room-temperature Hall measurement, which agrees very well with the above result.

In conclusion, we have demonstrated an experimental method for measuring the doping density in thin-sheet semiconductor material. The voltage dependence of the effective barrier height seen by the electrons going out of the quantum well is also determined experimentally.

Acknowledgments: This work is supported by the Advanced Research Projects Agency (ARPA), and by the US Air Force Office of Scientific Research.

4 November 1994
Electronics Letters Online No: 19950180

Y. Xu, A. Shakouri and A. Yariv (*Department of Applied Physics, California Institute of Technology, Pasadena, CA 91125, USA*)

T. Krabach and S. Dejewski (*303-210, Jet Propulsion Laboratory, California Institute of Technology, Pasadena, CA 91125, USA*)

References

1 SZE, S.M.: 'Physics of semiconductor devices' (John Wiley & Sons, New York, 1981)
2 LEVINE, B.F., BETHEA, C.G., HASNAIN, G., SHEN, V.O., PELVE, E., ABBOTT, R.R., and HSIEH, S.: 'High-sensitivity low dark current 10 μm GaAs quantum-well infrared photodetectors', *Appl. Phys. Lett.*, 1990, **56**, pp. 851–853
3 ANDREWS, S.R., and MILLER, B.A.: 'Experimental and theoretical studies of the performance of quantum-well infrared photodetectors', *J. Appl. Phys.*, 1991, **70**, pp. 993–1003
4 LEVINE, B.F., BETHEA, C.G., CHOI, K.K., WALKER, J., and MALIK, R.J.: 'Tunneling lifetime broadening of the quantum well intersubband photoconductivity spectrum', *Appl. Phys. Lett.*, 1988, **53**, pp. 231 233
5 XU, Y., SHAKOURI, A., YARIV, A., KRABACH, T., and DEJEWSKI, S.: To be published
6 LEE, C.Y., TIDROW, M.Z., CHOI, K.K., CHANG, W.H., and EASTMAN, L.F.: 'Activation characteristics of a long wavelength infrared hot-electron transistor', *Appl. Phys. Lett.*, 1994, **65**, pp. 442–444

Enhancement of potential barrier height by superlattice barriers in the InGaAsP/InP materials system

R.V. Chelakara, M.R. Islam and R.D. Dupuis

Indexing terms: Semiconductor superlattices, Band structure, Tunnelling

The authors have calculated the electron wave reflectivities for a variety of superlattice barriers in the InAlAs/InGaAsP/InP materials system. For an optimised superlattice barrier, we have calculated an effective barrier height of more than five times the classical barrier height available in this system. The significant improvement in the potential barrier height implies that the overflow leakage of hot electrons from the active layer to the cladding layer generated by the Auger effect can be suppressed, thereby improving the threshold current and the temperature characteristics of lasers in this system.

In 1973, Tsu and Esaki analysed the tunnelling phenomena for a one-dimensional semiconductor superlattice [1]. Since then, many semiconductor devices relying on the properties of superlattices have been proposed. For example, the use of a superlattice barrier (SLB) was proposed to effectively enhance the barrier height of a heterojunction, thereby reducing the number of injected carriers overflowing from the active layer into the cladding layer of a laser diode [2]. At high temperatures ($T > 300$K), high-power laser operation is often limited by the carrier overflow at the heterojunction. The use of superlattice barriers in laser structures has been previously studied in laser structures and has been shown to be effective in the InAlGaP system [3] and also in the InGaAsP system [4].

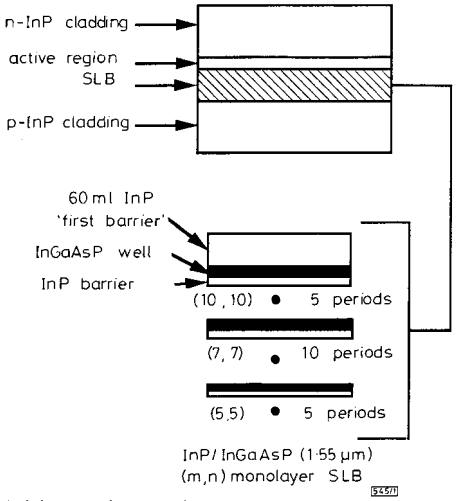

Fig. 1 *Schematic diagram of 20-period modulated InP/InGaAsP SLB structure*